ELSEVIER

Marine Chemistry 74 (2001) 261–278

MARINE CHEMISTRY

www.elsevier.nl/locate/marchem

Sulfur and iron speciation in surface sediments along the northwestern margin of the Black Sea

Jeroen W.M. Wijsman[a], Jack J. Middelburg[a,*], Peter M.J. Herman[a], Michael E. Böttcher[b], Carlo H.R. Heip[a]

[a] *Netherlands Institute of Ecology, P.O. Box 140, NL-4400 AC Yerseke, Netherlands*
[b] *Max-Plank-Institute for Marine Microbiology, Department of Biogeochemistry, Celsiusstr. 1, D-28359 Bremen, Germany*

Received 28 July 2000; received in revised form 19 February 2001; accepted 20 February 2001

Abstract

The speciation of sedimentary sulfur (pyrite, acid volatile sulfides (AVS), S^0, H_2S, and sulfate) was analyzed in surface sediments recovered at different water depths from the northwestern margin of the Black Sea. Additionally, dissolved and dithionite-extractable iron were quantified, and the sulfur isotope ratios in pyrite were measured. Sulfur and iron cycling in surface sediments of the northwestern part of the Black Sea is largely influenced by (1) organic matter supply to the sediment, (2) availability of reactive iron compounds and (3) oxygen concentrations in the bottom waters. Biologically active, accumulating sediments just in front of the river deltas were characterized by high AVS contents and a fast depletion of sulfate concentration with depth, most likely due to high sulfate reduction rates (SRR). The $\delta^{34}S$ values of pyrite in these sediments were relatively heavy (−8‰ to −21‰ vs. V-CDT). On the central shelf, where benthic mineralization rates are lower, re-oxidation processes may become more important and result in pyrite extremely depleted in $\delta^{34}S$ (−39‰ to −46‰ vs. V-CDT). A high variability in $\delta^{34}S$ values of pyrite in sediments from the shelf-edge (−6‰ to −46‰ vs. V-CDT) reflects characteristic fluctuations in the oxygen concentrations of bottom waters or varying sediment accumulation rates. During periods of oxic conditions or low sediment accumulation rates, re-oxidation processes became important resulting in low AVS concentrations and light $\delta^{34}S$ values. Anoxic conditions in the bottom waters overlying shelf-edge sediments or periods of high accumulation rates are reflected in enhanced AVS contents and heavier sulfur isotope values. The sulfur and iron contents and the light and uniform pyrite isotopic composition (−37‰ to −39‰ vs. V-CDT) of sediments in the permanently anoxic deep sea (1494 m water depth) reflect the formation of pyrite in the upper part of the sulfidic water column and the anoxic surface sediment. The present study demonstrates that pyrite, which is extremely depleted in ^{34}S, can be found in the Black Sea surface sediments that are positioned both above and below the chemocline, despite differences in biogeochemical and microbial controlling factors.

Keywords: Euxinic basin; Sulfur; Iron; Diagenesis; Pyrite; Sulfur isotopes; Black Sea; Continental shelf

---

1. Introduction

River deltas and continental shelf areas play an important role in the global cycles of sulfur and iron

---

[*] Corresponding author. Tel.: +31-113-577-476; fax: +31-113-573-616.
E-mail address: middelburg@cemo.nioo.knaw.nl (J.J. Middelburg).

0304-4203/01/$ - see front matter
PII: S0304-4203(01)00019-6

and are important sites for the formation and burial of authigenic iron sulfides (Berner, 1982; Jørgensen, 1982; Lin and Morse, 1991). This is due to high rates of organic matter fluxes to the sediments in combination with the input of reactive iron through rivers (e.g., Lin and Morse, 1991). With increasing load of particles with associated reactive organic matter to the sediment, the relative importance of sulfate reduction usually increases (Canfield, 1989; Thamdrup and Canfield, 1996; Wijsman et al., 2001a). Sulfate reduction is, therefore, the major mineralization pathway in sediments of productive coastal marine systems, accounting for 10–90% of the total organic matter degradation (Jørgensen, 1977, 1982; Henrichs and Reeburgh, 1987; Canfield et al., 1993b; Thamdrup and Canfield, 1996; Kostka et al., 1999).

Dissolved hydrogen sulfide that is produced during bacterial dissimilatory sulfate reduction may quickly react with sedimentary reactive iron compounds to form iron monosulfide, FeS_x, (Rickard, 1995), which can further react with dissolved sulfide, elemental sulfur or polysulfides (Berner, 1970; Luther, 1991; Rickard, 1997) to form pyrite (FeS_2). This immobilization of free sulfide within the sediment has major consequences for the cycling of iron and sulfur. Transport processes and turnover rates are significantly reduced by the formation of solid-phase iron sulfides. Moreover, the formation of iron sulfides and the subsequent burial in the sediment has been recognized as the dominant pathway for the permanent removal of sulfur and iron (Berner, 1982; Berner and Raiswell, 1983). Since hydrogen sulfide ($\Sigma H_2S \equiv H_2S_{(aq)} + HS^- + S^{2-}$) dissolved in the pore waters is toxic for many macrofaunal species (e.g., Bagarinao, 1992), the fixation of H_2S through the formation of metal sulfides is also an important detoxifying mechanism for the macrofauna community.

In the absence of sufficient sedimentary reactive iron, H_2S can diffuse into underlying sediments or the water column (Passier et al., 1999), can be chemically or microbially reoxidized to sulfur intermediates (elemental sulfur, thiosulfate, sulfite) or sulfate (Fossing and Jørgensen, 1990; Zhang and Millero, 1993) or react with organic matter (e.g., Sinninghe Damste and De Leeuw, 1990). Additionally, bioturbating organisms can transport iron sulfide minerals from the reduced to the oxidized part of the sediments, where they are subsequently re-oxidized (Berner and Westrich, 1985; Aller, 1988; Aller and Rude, 1988). Thus, benthic organisms might enhance the recycling of sulfur and iron within the sediments by their bioturbating and bio-irrigating activities. Oxygen has a direct effect on sulfur and iron cycling through re-oxidation but also an indirect effect by its influence on the biomixing and bio-irrigating activity of the macrofauna that, in turn, depend on oxygen to respire.

It has been shown that most of the H_2S produced in the sediments is not permanently buried but reoxidized (Jørgensen, 1977). Besides diagenetic pyrite formation in the sediment, syngenetic precipitation in the anoxic water column has been shown to significantly contribute to sedimentary pyrite in the Black Sea (Muramoto et al., 1991; Fry et al., 1991; Raiswell and Canfield, 1998; Neretin et al., 2001).

The overall effect of early diagenetic reactions is not only reflected in the depth distributions of various dissolved and particulate sulfur and iron compounds within the sediment (e.g., Jørgensen, 1983) but also in the stable isotopic composition of metal sulfides, specifically pyrite and AVS (e.g., Goldhaber and Kaplan, 1974). The bacterial dissimilatory reduction of sulfate is associated with a significant discrimination of the stable sulfur isotopes ^{34}S and ^{32}S, leading to an enrichment of the lighter isotope in the H_2S produced (e.g., Chambers and Trudinger, 1979). Since no significant further isotope discrimination occurs upon iron sulfide formation (Price and Shieh, 1979; Böttcher et al., 1998a), the overall isotopic composition of the metabolic product H_2S should be preserved in the pyrite fraction. Therefore, the sulfur isotope ratios of sedimentary sulfur species in marine sediments have been found to be extremely useful in the characterization of biogeochemical processes in the coupled sulfur–carbon–iron cycles during early diagenesis (e.g., Goldhaber and Kaplan, 1974; Raiswell, 1997; Böttcher et al., 1998b, 2000; Passier et al., 1999). Most previous studies on the sulfur isotope geochemistry of Black Sea sediments were related to the water column or sediments deposited below the chemocline (Sweeney and Kaplan, 1980; Muramoto et al., 1991; Fry et al., 1991; Calvert et al., 1996; Lyons, 1997; Neretin et al., 1998, 2001). Pyrite which is found in the water column and the surface sediments in the anoxic part is extremely depleted by up to 62‰ compared to coexisting sulfate (e.g., Fry et al., 1991; Lyons, 1997; Neretin et al., 1998). However, experiments with sulfate-reducing bacteria isolated from the Black Sea water column yielded an isotope fractionation of only about 30‰ (Fry et al., 1991). This discrepancy has been attributed to contributions from the oxidative part of the sulfur cycle (Canfield and Thamdrup, 1994) but is still a matter of debate (Fry et al., 1991; Neretin et al., 2001).

In the present study, we document the distribution of iron sulfur speciation and the sulfur isotope composition of pyrite in surface sediments of the northwestern Black Sea along a transect from the coastal area, just in front of the river deltas, down to the anoxic deep sea. It was the aim to provide additional information on the influence of depositional environments on the formation of and sulfur isotope partitioning into early diagenetic and syngenetic pyrite.

2. Study area

The Black Sea is the worlds largest anoxic basin with a permanent reservoir of hydrogen sulfide in the water column at depths $> \sim 100$ m (Sorokin, 1983; Sweeney and Kaplan, 1980; Codispoti et al., 1991). It has been the subject of intensive study concerning the cycling of iron and sulfur (e.g., Berner and Raiswell, 1983; Berner, 1984; Calvert and Karlin, 1991; Middelburg et al., 1991; Lyons and Berner, 1992; Lyons, 1997; Wilkin et al., 1997; Wijsman et al., 2001b). The Black Sea is often seen as the modern equivalent of ancient euxinic basins with pyrite formation and sulfide oxidation processes existing in the upper part of the sulfidic water column of the deep-sea (Goldhaber and Kaplan, 1974; Calvert and Karlin, 1991; Luther et al., 1991; Jørgensen et al., 1991). Consequently, most previous studies concerning the iron and sulfur cycling in the Black Sea focused on the deep basin.

Three major rivers (Danube, Dniester and Dnieper), accounting for 76% of the total river input into the whole Black Sea (Tolmazin, 1985; Mee, 1992; Fabry et al., 1993), discharge their water onto the northwestern shelf, which represents only 17% of the total Black Sea area (Tolmazin, 1985; Wijsman et al., 1999). The presence of these rivers on one side and the anoxic deep sea on the other introduces strong gradients across the northwestern shelf that could potentially affect the cycling of iron and sulfur within the sediments. The rivers discharge large amounts of nutrients and particulate and dissolved organic matter to the shelf. Consequently, sediment accumulation and the benthic mineralization rates in the area just in front of the river mouths are much higher compared to the offshore areas (Wijsman et al., 1999). Large rivers like the Danube are also a major source of reactive iron to continental shelf sediments (Martin and Windom, 1991; Guieu et al., 1998). In the Black Sea, some of this reactive iron is re-allocated from the shelf to the deep-sea sediments through pyrite formation in the water column of the deep sea (Wijsman et al., 2001b). The oxygen concentration of the bottom water on the northwestern shelf is also variable. Due to upwelling/downwelling, internal waves and seasonal and long-term changes in mean circulation, the oxic–anoxic interface migrates over the shelf edge (Dimitrov et al., 1987; Shaffer, 1986; Lyons et al., 1993). As a consequence, the bottom-water oxygen concentration in the area near the oxic–anoxic interface fluctuates between fully oxic and anoxic–sulfidic. Moreover, oxygen depletions could occur in the shallow coastal waters as a result of high degradation rates in the sediment after a phytoplankton bloom in combination with a temperature stratification of the water column (Zaitsev, 1993).

3. Material and methods

3.1. Sampling locations

Sediment was collected from nine stations in the northwestern part of the Black Sea in May 1997 (Fig. 1; Table 1). Stations 2, 9, 10, 24 and 22 were positioned on a transect ranging from high organic loading in the shallow coastal waters to low organic loading in the permanently anoxic deep-sea. The coastal station 13 was located in front of the mouth of the river Dniester. Station 16 was situated in the

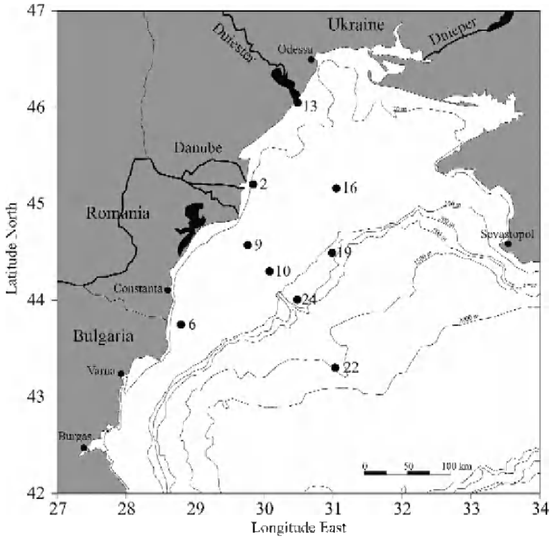

Fig. 1. Locations of the sampling stations in the northwestern part of the Black Sea.

northern part of the central shelf and is influenced by (the discharge of) the Danube river (Wijsman et al., 1999), while station 6 in the southern part of the central shelf is less influenced by the Danube river. Stations 19 and 24 were positioned at the shelf-edge, near the interface between oxic and anoxic bottom water. Station 22 was located in the anoxic deep sea at a depth of 1494 m. Sediment was sampled at all stations using a Reineck box-corer (60 × 30 × 30 cm).

3.2. Pore water collection and analysis

Sediment cores were sub-sampled from the box-corer using Plexiglas core tubes (10.3 cm i.d., 50 cm length) and closed with rubber stoppers. The cores were transferred into a N_2 gas filled glove box (O_2 concentration < 500 ppm) through an air lock at the bottom of the box and sectioned as follows 0–0.5, 0.5–1, 1–2, 2–3, 3–4, 4–5, 5–7, 7–9, 9–11, 14–16, 19–21, 24–26 and 29–31 cm. Pore water was obtained by squeezing over a 0.45-μm filter using manually operated Teflon squeezers at a maximum pressure of 1 bar N_2 gas inside the glove box. A sub-sample of 1 ml filtered pore water was collected and preserved in anoxic $Zn(Ac)_2$ (50 μl; 1 M) for H_2S determination (Cline, 1969) and stored frozen until analysis. Another sub-sample of 3 ml was acidified with H_2SO_4 (100 μl; 7 N) and analyzed within 1 month for total dissolved iron concentration using a graphite furnace atomic absorption spectrometer with Zeeman background correction. Some complexed Fe(III) may contribute to the measured concentration of total dissolved iron. SO_4^{2-} concen-

Table 1
Characteristics of sampling stations in the northwestern part of the Black Sea

Station	Area	Location		Depth (m)	Oxygen (μM)	Temp (°C)	Org. C (%)[a]	Total S (μmol g^{-1})[a]	Total Fe (μmol g^{-1})[a]	SCOC (mmol O_2 m^{-2} day^{-1})
		Latitude	Longitude							
13	Delta	46°03′N	30°29′E	13	350	8.4	0.64	72	202	26.3
2	Delta	45°12′N	29°51′E	26	207	6.5	2.15	244	807	37.9
6	Central shelf	43°45′N	28°48′E	52	285	6.8	0.84	70	205	13.5
16	Central shelf	45°10′N	31°03′E	54	314[b]	5.5[b]	2.78	46	123	10
9	Central shelf	44°34′N	29°46′E	57	243	6.6	1.71	194	504	11.6
10	Central shelf	44°18′N	30°05′E	72	284	6.6	2.93	115	200	11
19	Shelf edge	44°29′N	31°00′E	120	126[b]	7.7	2.53	200	486	6.1
24	Shelf edge	44°00′N	30°29′E	137	190[b]	7.5	1.56	164	368	3.7
22	Deep-sea	43°18′N	31°02′E	1494	0	9	4.64	488	298	n.d[c]

[a] Upper 16 cm of the sediment.
[b] Measured in the bottom water from the box-corer.
[c] Not determined.

tration was measured spectrophotometrically in the remainder of filtered, acidified pore water using an autoanalyzer.

3.3. Solid phase analysis

The solid residues that remained after squeezing were put into diffusion-free bags and stored frozen for solid phase iron and sulfur analysis. All further processing of these solid residue samples were performed in a Coy anaerobic chamber (Coy Laboratory Products, Ann Arbor, MI) to prevent oxidation. The anaerobic chamber was filled with a mixture of H_2 gas (5%) and N_2 gas (95%). Any traces of oxygen were consequently removed by reaction with H_2 gas on a palladium catalyst. The oxygen concentration in the chamber was always less than 0.5 ppm.

Acid volatile sulfides (AVS), which include iron monosulfides ("FeS") and remaining dissolved hydrogen sulfide, were extracted from 0.5 g homogenized wet sediment samples by means of cold acid distillation (Fossing and Jørgensen, 1989) for 2 h in deoxygenated HCl (10 ml, 6 N). The liberated sulfide was stripped from the solution with N_2 gas and trapped in 10 ml deoxygenated $Zn(Ac)_2$ (0.1 M). At the end of the distillation, the ZnS concentration in the traps was measured using the methylene blue method (Cline, 1969).

For pyrite determination, 2–3 g wet sediment was dried 3 days in a hood at 40°C to oxidize the AVS to elemental sulfur (Henneke et al., 1991; Passier et al., 1999) and ground by mortar and pestle. The elemental sulfur produced by AVS oxidation, together with the elemental sulfur originally present in the sediment, were removed by double extraction with acetone (Passier et al., 1996). Pyrite was determined using the Cr(II) reduction method (Zhabina and Volkov, 1978; Fossing and Jørgensen, 1989; Canfield et al., 1986). About 10 mg of the dry, acetone-extracted sediment was digested in 16 ml of 1 M Cr^{2+} in 0.5 N HCl and 8 ml 12 N anoxic HCl. Hydrogen sulfide that evolved was quantified as it was for AVS. Additionally for pyrite sulfur isotope analysis ($\delta^{34}S_{pyrite}$), about 0.2 g acetone extracted sediment was exposed to a cold chromium reduction. The evolved hydrogen sulfide was trapped in $Zn(Ac)_2$ and subsequently converted to Ag_2S by addition of a slight excess of $AgNO_3$. The Ag_2S was collected on 0.45 μm filters, carefully washed and dried. The sulfur isotopic compositions was measured by means of combustion isotope-ratio-monitoring mass spectrometry (C-irmMS) using a Carlo Erba elemental analyzer connected to a Finnigan MAT 252 gas isotope mass spectrometer via a Finnigan Conflo II split interface (Böttcher et al., 1998a). $^{34}S/^{32}S$ ratios are expressed in the δ-notation relative to the Vienna Canyon Diablo Troilite (V-CDT) standard.

Sub-samples of 1 g wet sediment were extracted for elemental sulfur (S^0) determination. First, the samples were rinsed with anoxic sodium chloride (0.5 M) to remove the residual pore water sulfate. Then, elemental sulfur was extracted twice with deoxygenated methanol. The methanol mixture was analyzed for elemental sulfur by means of reverse-phase HPLC (Henneke et al., 1997). Total sulfur content of the sediment was determined on dried and homogenized samples with a Carlo Erba NA 1500 elemental analyzer using vanadium pentoxide as catalyst to ensure complete oxidation.

Dithionite extractable iron (FeD) was determined by adding 0.5–1 g wet sediment to 10 ml dithionite (sodium dithionite 50 g l^{-1} in 0.2 M sodium citrate/0.35 M acetic acid; pH = 4.8) in 20-ml glass vials (Kostka and Luther, 1994). Samples were vortex mixed and placed on a rotary shaker for 2 h. After extraction, the samples were filtered over a 0.45-μm filter and stored for 1 day to oxidize the dithionite and sulfite (Canfield et al., 1993a). The extracted iron was determined by the injection of 50 μl solution into 5 ml reducing HEPES (12 g HEPES plus 20 ml hydroxylamine [10 g/100 ml] l^{-1}, pH = 7.0). After 30 min, 300 μl Ferrozine (5 g l^{-1}) was added, and iron was determined spectrophotometrically after a minimum of 3 h for complete color development (Stookey, 1970; Canfield et al., 1993a). Dithionite was expected to extract both poorly and well-crystallized iron oxides (except magnetite), AVS-Fe, iron-containing carbonates and iron adsorbed onto sediment particles (Canfield et al., 1993a; Canfield, 1988). Additionally, there may be a small contribution of iron from silicate minerals (Raiswell et al., 1994). Porosity of the solid residue was calculated from water contents (weight loss on drying 105°C) assuming a sediment dry density of 2.55 g cm^{-3}.

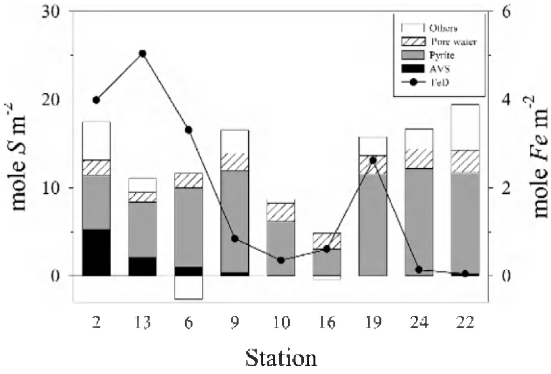

Fig. 2. Distribution of various sulfur species (stacked bars) and dithionite extractable iron (line graph) integrated over the upper 16 cm of the sediment. Others represent total sulfur minus AVS, pyrite and pore water sulfur (SO_4^{2-} and H_2S), and include elemental sulfur. Stations are ordered with a decreasing organic matter loading as implied by the sediment community oxygen consumption.

3.4. Sediment community oxygen consumption (SCOC)

Oxygen fluxes across the sediment water interface were measured by shipboard core incubations. Two Plexiglas core tubes (10.3 cm i.d.; 30 cm length) were sub-sampled from the box-corer and sealed with a lid containing a YSI 5739 oxygen electrode and a Teflon coated magnetic stirrer. The cores were incubated in the dark in a thermo-stated bath at in situ temperature for 4–8 h. SCOC was calculated by linear regression of the oxygen concentration of the overlying water vs. incubation time. A more detailed description of the flux chamber measurements is given by Wijsman et al. (1999).

4. Results

4.1. Sulfur and iron species inventory

Depth-integrated data for the various sulfur fractions (AVS, pyrite, sulfate and others) and dithionite extractable iron (FeD) are presented in Fig. 2. The stations are arranged with respect to a decreasing SCOC (Table 1), which is an indicator for the depth-integrated rate of carbon mineralization in sediments (Heip et al., 1995). For each station, the data are integrated over the upper 16 cm of the sediment column, which is the maximum depth for which data are available for all stations. Pyrite sulfur was the

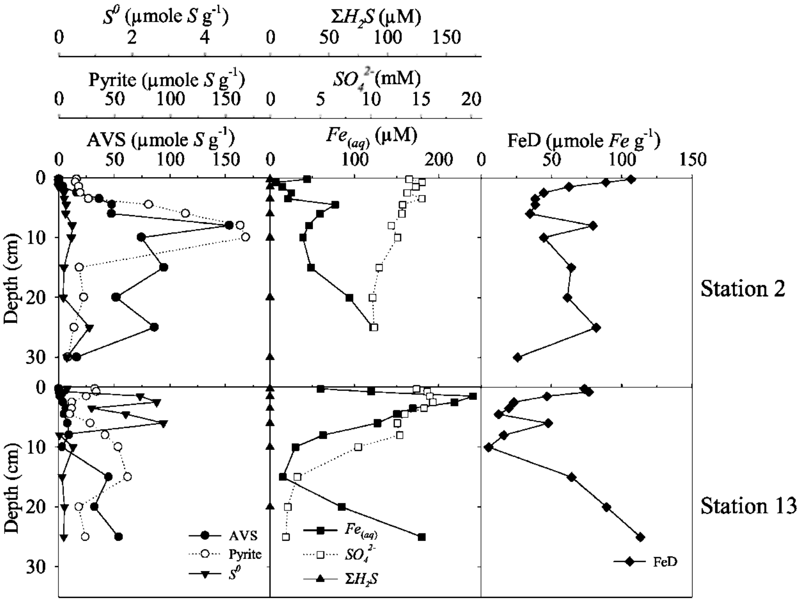

Fig. 3. Concentration versus depth profiles of AVS, pyrite, S^0, dissolved iron ($Fe_{(aq)}$), SO_4^{2-}, ΣH_2S and dithionite extractable iron (FeD) for stations 2 and 13 located in front of river deltas.

major sulfur phase at all stations, accounting on average for 67% of the total sulfur pool. Highest pyrite contents were found at the central shelf station 9 (11.6 mol S m^{-2}), stations 19 and 24 near the oxic–anoxic interface (11.6 and 12.1 mol S m^{-2}, respectively) and at the deep-sea station 22 (11.5 mol S m^{-2}). AVS contents were highest in the accumulating, high oxygen demand stations (2 and 13) in front of the rivers Danube and Dniester (5.3 and 2.1 mol S m^{-2}, respectively) and decreased offshore. Pore water SO_4^{2-} inventories ranged from 1.1 mol S m^{-2} at station 13 to 2.5 mol S m^{-2} at station 22, which is partly due to differences in porosity. The low SO_4^{2-} concentrations at the coastal stations 2 and 13 are caused by the low salinity in this area and through sulfate reduction within the sediment. The sulfur fraction indicated by 'Others' that includes organic sulfur is calculated by difference from the total sulfur content and pyrite, AVS and SO_4^{2-}. Due to analytical uncertainty and propagation of errors, this resulted in negative concentrations at stations 6 and 16 (−0.26 and −0.04 mol S m^{-2}, respectively). The fraction of elemental sulfur was always less than 1.5% of the total sulfur content and was assigned to 'Others'. Dithionite extractable iron (FeD) includes oxidized forms of iron that are available for iron

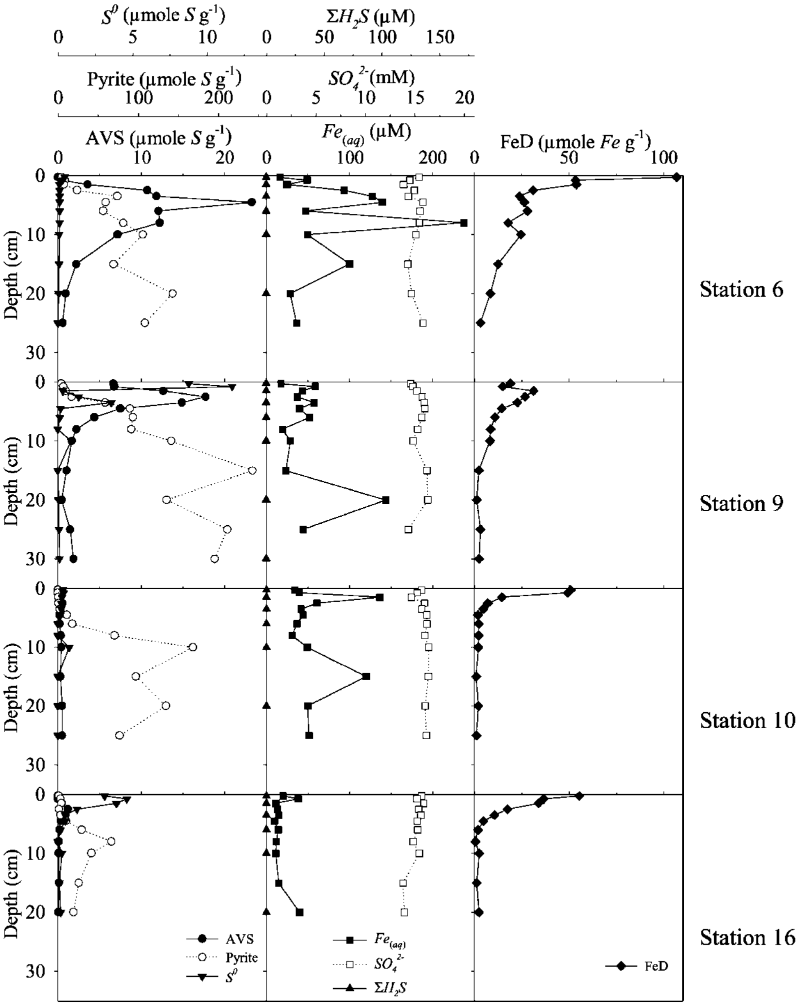

Fig. 4. Concentration vs. depth profiles of AVS, pyrite, S^0, dissolved iron ($Fe_{(aq)}$), SO_4^{2-}, ΣH_2S and dithionite extractable iron (FeD) for stations 6, 9, 10 and 16 located in central part of the continental shelf.

reduction and iron in the form of AVS. FeD was highest in the coastal stations (2, 13 and 6) and decreased offshore. Remarkably high FeD concentrations were found at stations 19, which was located near the oxic–anoxic interface.

4.2. Down core distribution of sulfur and iron species

The pore water profiles of the accumulating, high oxygen demand river delta sediments (stations 2 and 13) showed a clear decrease in SO_4^{2-} from 15 mM near the sediment–water interface to 10 and 2 mM at 25 cm depth, respectively (Fig. 3). At both stations, the decline was strongest at depths more than 10 cm. This decrease in SO_4^{2-} concentration with depth in the sediment suggests relatively high rates of sulfate reduction at these stations. In spite of these high sulfate reduction rates, no free sulfide was observed in the pore water. The concentrations of AVS in these delta sediments were relatively high (up to 153 and 54 μmol S g^{-1} for stations 2 and 13, respectively). The AVS remained high at depth in the sediment and was not converted to pyrite. Due to oxidation and conversion into pyrite, the AVS concentrations near the sediment–water interface were very low at both stations. Relatively high amounts of pyrite were observed near the sediment–water interface of both stations. At coastal stations with a relatively high biomass of deposit feeders (Wijsman et al., 1999), pyrite can be transported from the deeper sediment layers to the sediment–water interface. Since pyrite is less vulnerable to oxidation than AVS, it will not be completely oxidized. A remarkable feature in the pyrite profiles at stations 2 and 13 (Fig. 3) was the abrupt decrease at depths of approximately 15 and 20 cm, respectively. Since it is not likely that pyrite is oxidized at these depths, we suggest this decrease reflects non-steady state deposition due to fluctuations in bottom-water salinities or oxygen contents or in delivery of carbon and sediment. Moreover, the dissolved iron and FeD profiles show that reactive iron oxides were still present at these sediment depths.

The invariant profiles for sulfate that were observed at the central shelf stations (Fig. 4) indicate that the net sulfate reduction (i.e., sulfate reduction–sulfide oxidation) was low compared to the delta stations. Also, sulfide was below the detection limit (< 1 μM). The profiles of S^0, AVS and pyrite display classical patterns for coastal sediments. The

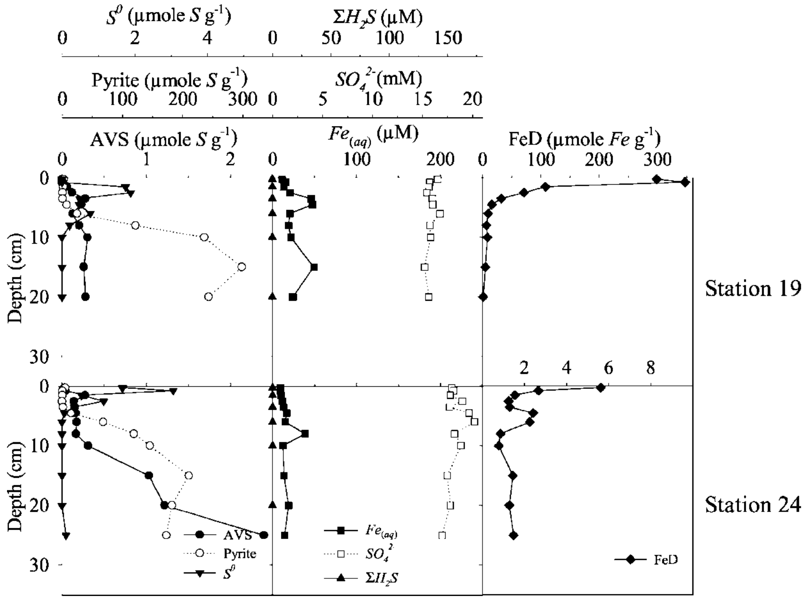

Fig. 5. Concentration versus depth profiles of AVS, pyrite, S^0, dissolved iron ($Fe_{(aq)}$), SO_4^{2-}, ΣH_2S and dithionite extractable iron (FeD) for stations 19 and 24 located in at the shelf-edge, near the interface between oxic and anoxic bottom water. Mind the different scales for FeD.

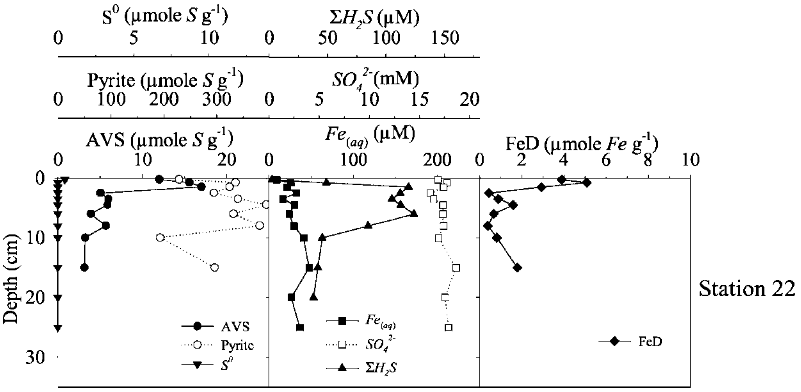

Fig. 6. Concentration vs. depth profiles of AVS, pyrite, S^0, dissolved iron (Fe$_{(aq)}$), SO$_4^{2-}$, ΣH$_2$S and dithionite extractable iron (FeD) for the deep-sea station 22.

AVS profiles are characterized by a subsurface peak at a depth of 2–5 cm, which is the depth where "FeS" is formed through the reaction of sulfide with reactive iron. In the more oxidized conditions near the sediment–water interface, AVS is either produced at low levels, or consumed by oxidation, which is reflected by a peak in S^0. At greater depth in the sediments, FeS reacts further to pyrite. As a result, the pyrite concentration increased from a depth of about 2–5 cm. The strong decrease of dithionite extractable iron in the upper part of the sediment suggests a high activity of iron reduction at this depth. However, this is not reflected in a clear peak in dissolved iron. Dissolved iron produced by iron reduction was likely removed by secondary reactions such as iron sulfide formation and iron oxidation.

The profiles of dithionite extractable iron were very different between the two stations located near the oxic–anoxic interface (Fig. 5). Station 19 (120 m) showed a distinct peak in FeD at the sediment–water interface of more than 300 μmol Fe g^{-1}, while this peak was absent at the slightly deeper station 24 (137 m). Apparently dissolved iron that is produced by iron reduction was efficiently oxidized at or near the sediment–water interface of station 19, while at station 24 iron was probably lost from the sediments by diffusion into the water column. The uniform distribution of sulfate concentration with sediment depth, the low Fe sulfide concentrations and the absence of free sulfide in the pore water suggest that the net effect of sulfate reduction was relatively limited in this area. This is confirmed by the low respiration rates at these stations (Table 1). The pyrite profiles corresponded to the profiles observed at the central shelf stations, with an increase from < 15 μmol S g^{-1} in the upper 5 cm to a maximum value of 200–300 μmol S g^{-1} at depths of more than 10 cm. AVS concentrations at these stations were very low (< 3 μmol S g^{-1}) and increased with depth in the sediment. The peak in elemental sulfur near the sediment–water interface reflected oxidation of reduced sulfur.

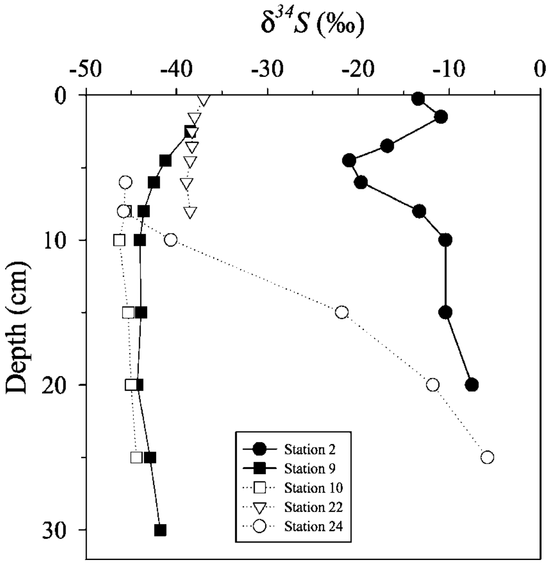

Fig. 7. Distribution of δ^{34}S values of pyrite versus sediment depth at stations 2, 9, 10, 22 and 24.

At the deep-sea station 22, H_2S was observed in the pore water (Fig. 6). The decreased concentration near the sediment–water interface might be due to oxidation during sampling or related to iron sulfide formation near the sediment–water interface. The majority of this H_2S was probably not produced

Table 2
Compilation of $\delta^{34}S$ data (‰) for sulfur species from the water column, sediment traps and surface sediments of the Black Sea.

Station	Water depth (m)	Depth	$\delta^{34}S$ (‰)				Reference
			Sulfate	ΣH_2S	S^0 (+polysulfide)	$S_2O_3^{2-}$ (+SO_3^{2-})	
Water column							
St.6	401	> 324 m		−39.5 to −40.3			(1)
St.7	1204	> 472 m		−38.7 to −39.9	−39.7		(1)
1136	2000	0–200 m	+18.5 ($\sigma = 0.3$)				(2)
		> 200 m	+19.4 ($\sigma = 0.7$)	−39.6 ($\sigma = 0.7$)			(2)
St.8	2045	> 475 m		−39.4 to −40.1	−31.3 to −39.3	−38.5	(1)
1135	2050	0–200 m	+18.4 ($\sigma = 0.2$)				(2)
		> 200 m	+19.6 ($\sigma = 0.5$)	−40.1 ($\sigma = 0.6$)			(2)
BS2-1	2128	0–300 m		−40 to −38			(3)
		> 300 m		−40.5[a]			(3)
BS2-2	2130	0–300 m		−41 to −37			(3)
		> 300 m		−40.5[a]			(3)
BS2-3	2220	0–300 m		−41 to −35			(3)
		> 300 m	+19.5[b]	−40.5[a]			(3)
			Sulfate	ΣH_2S	Pyrite	TIRS[c]	
Sediment traps							
BSC2	~ 2100	1065 m			−37.6 ($\sigma = 1.6$)[d]		(4)
BSK2S	~ 2100	477 m			−32.7[d]		(4)
Sediments							
Station 2	26	0–21 cm			−13.7 ($\sigma = 4.6$)		(5)
Station 9	57	2–31 cm			−42.5 ($\sigma = 1.8$)		(5)
Station 10	72	7–26 cm			−45.3 ($\sigma = 0.7$)		(5)
Station 24	137	5–26 cm			−28.6 ($\sigma = 17.8$)		(5)
15	198	Slope			−27.6 ($\sigma = 1.1$)		(6)
Shelf	< 200 m	Surface[e]	+19.6 ($\sigma = 1.0$)		−30.7 ($\sigma = 14.5$)		(7)
Deep Sea	> 200 m	Surface[f]	+20.4 ($\sigma = 0.5$)		−33.4 ($\sigma = 3.3$)		(7)
St.6	394	2–4 cm		−38.7			(8)
St.7	1204	2–10 cm		−36.1			(8)
Station 22	1494	0–9 cm			−38.2 ($\sigma = 0.6$)		(5)
1136	2000	Surface[f]				−27.0	(2)
St.8	2045	10–18 cm		−40.4			(8)
1135	2050	Surface[f]				−27.4	(2)
9	2094	Unit 1			−37.3 ($\sigma = 0.7$)[d]		(6)
1474K	2117	Unit 1			−33.5 ($\sigma = 1.2$)	−29.4 ($\sigma = 0.1$)	(9)
14	2218	Unit 1			−37.0 ($\sigma = 1.1$)[d]		(6)
BS4-14GC	2218	Unit 1			−33.6 ($\sigma = 0.5$)	−27.3 ($\sigma = 0.6$)	(9)

Data are derived from: (1) Neretin et al. (1998, unpublished data), (2) Sweeney and Kaplan (1980), (3) Fry et al. (1991), (4) Muramoto et al. (1991), (5) This study, (6) Lyons (1997), (7) Vaynshteyn et al. (1986), (8) Neretin et al. (2001) and (9) Calvert et al. (1996).

[a] Average value for deep water (> 300 m) at all 3 stations.

[b] Water sample taken at 500 m depth.

[c] TIRS: Total reduced inorganic sulfur.

[d] Chromium reducible sulfur fraction.

[e] Surface sediments (0–10 cm). Data averaged for all stations.

[f] Surface sediments, depth not specified.

locally by sedimentary sulfate reduction since there was no sulfate gradient. Dithionite-extractable iron at station 22 was mainly composed of AVS. Although the majority of the iron sulfides reach the sediment in the form of pyrite, there is also a small fraction of FeS reaching the sediment or formed in the sediments. During burial in the sediment, this FeS is converted to pyrite.

4.3. Sulfur isotopic composition of sedimentary pyrite

The heaviest δ^{34}S values (-13.7‰; $\sigma = 4.6$‰) were observed at station 2 in front of the Danube delta (Fig. 7). Assuming an isotopic composition for dissolved sulfate of about $+19$‰ (Sweeney and Kaplan, 1980) for the near bottom water at the continental shelf, this corresponds to an apparent isotopic fractionation of about 32‰. At the central shelf stations (9 and 10), the δ^{34}S values of pyrite were much lower (-46.3‰ to -38.5‰), resulting in apparent isotope fractionation between 57‰ and 65‰. At station 9, pyrite was slightly enriched in ^{34}S towards the sediment–water interface. The isotope values in the upper 10 cm of station 24, located near the interface between oxic and anoxic bottom waters, were similar to those observed in the central shelf stations. At greater depth, the δ^{34}S value of increased rapidly up to -5.8‰ at 25 cm depth. The δ^{34}S values at the deep sea station 22 ranged from -37.0‰ to -38.9‰. This is similar to previous data reported for Unit 1 sediments in the Black Sea (Table 2) and corresponds to δ^{34}S values between -35‰ and -40‰ that are reported for H_2S near the chemocline (Fry et al., 1991; Lyons, 1997) or in the deeper part or the anoxic water column (Neretin et al., 1998), as well as pore-water H_2S from deep sea sediments (Neretin et al., 2001). The isotopic composition of pyrite corresponds to an apparent isotopic fractionation factor of about 57‰.

5. Discussion

5.1. Downcore distribution of iron and sulfur species

The presence of large rivers discharging high amounts of suspended solids and nutrients (Popa, 1993) cause clear gradients in sedimentation, organic loading and iron input into the sediments of the northwestern continental shelf of the Black Sea. This is also reflected in the depth distribution of the various sulfur and iron fractions in the sediments. The delta areas, with sedimentation rates of about 1 cm year^{-1} (Wijsman et al., 1999) are characterized by relatively high rates of benthic mineralization (Table 1). As a result of high sulfate reduction rates, the sulfate concentration decreases with depth in the sediment at both delta stations (2 and 13). The break in sulfate profiles that is observed at a depth of 10 cm at station 13 could mark the maximum depth of bio-irrigation in these sediments (Goldhaber et al., 1977). However, we suggest that this break is caused by enhanced rates of sulfate reduction at depths greater than 10 cm. This is supported by the relatively high concentrations of AVS at these depths, which are not (yet) converted to pyrite. According to Boesen and Postma (1988), Middelburg (1991), Gagnon et al. (1995), Hurtgen et al. (1999) and others, preservation of FeS in modern sediments occurs in rapidly accumulating sediments and can be attributed to a lack of elemental sulfur, polysulfides or hydrogen sulfide that are necessary to transform FeS to FeS_2. However, this does not seem to be the case at these stations, where elemental sulfur is observed over the entire measured depth range. Besides the presence of elemental sulfur, polysulfides or hydrogen sulfide, the transformation of FeS to pyrite requires time (Middelburg, 1991). According to Berner (1970), the process occurs on a timescale of years. Apparently, pyrite formation in these active sediment layers is not completed yet, which is also reflected in the abrupt decrease in the pyrite concentrations at 15 (station 2) and 20 cm (station 13). We suggest that there is an active layer present at a depth of 10–20 cm at both delta stations with high concentrations of labile carbon, consequent high rates of sulfate reduction and AVS formation and with still substantial concentrations of reactive iron oxides (Fig. 3). This is a clear example of non-steady state deposition because these sediments are covered with less active sediments with higher pyrite concentrations.

In comparison to the Delta stations, the central shelf stations are characterized by lower carbon loading to the sediment, as is reflected in lower oxygen uptake measurements (Table 1). The depth profiles of the various sulfur and iron fractions show classical patterns that could largely be described by the use of a steady state diagenetic model (Wijsman et al., 2001a). There are exponential decreases in FeD with depth in the upper part of the sediment, subsurface peaks in AVS at depths of 2–5 cm, increases in pyrite and peaks in S^0 at sediment water interfaces due to oxidation. These sulfur and iron profiles were consistent among the stations, but the total amount varies between the stations. The maximum concentrations of AVS at stations 6 and 9, which are located closer to the coast, are higher (23.3 and 17.7 μmol S g^{-1}, respectively) than the more offshore stations 10 and 16 (0.6 and 1.2 μmol S g^{-1}, respectively). This difference could partly be explained by differences in carbon loading, but also factors such as the sediment accumulation rate and availability of reactive iron and mixing processes by bioturbating and bio-irrigating benthic organisms in the sediment could cause this. Middelburg (1991), Kostka and Luther (1994), Gagnon et al. (1995) and Lyons (1997) have demonstrated that high AVS concentrations occur in sediments with high deposition rates.

The organic loading to the sediments at the stations located near the shelf-edge is low compared to the other shelf stations. This is reflected in low concentrations of AVS. The sulfur and iron cycling in these sediments is to a large extent influenced by changes in the oxygen concentration in the bottom water, which is highly variable in this region (Shaffer, 1986; Kempe et al., 1990). The shallowest station 19 is characterised by very high concentrations of FeD in the upper part of the sediment column. This suggests intensive recycling of iron by re-oxidation reactions (Wijsman et al., 2001b). This is clearly not the case at station 24 where FeD concentrations in the upper sediments are two orders of magnitude lower. Although the concentration of AVS is low at station 24 (< 2.5 μmol S g^{-1}), it increases with depth in the sediment. This might be related to a recent shift from anoxic to oxic conditions of the bottom water. During anoxia, AVS could also exist near the sediment water interface. During the oxic conditions this AVS becomes readily oxidized. Alternatively, it might reflect a drop in sediment accumulation rate with time.

The processes in the water column largely determine iron and sulfur in the sediments of the deep-sea station 22. The flux of labile organic matter to these sediments is very low (Calvert et al., 1996) and consequently the rate of sulfate reduction in these sediments is also very low. According to the depth profile of AVS, some of the FeS that is deposited on the sediment is converted to pyrite in the upper centimeters. It is not likely that intermediate sulfur species are present and diagenetic pyrite could only be formed through the reaction of FeS with H_2S (Rickard, 1997). In the euxinic Black Sea, pyrite is formed in the upper part of the water column through the reaction of reactive iron with sulfide and most of the sedimentary pyrite is syngenetic (Goldhaber and Kaplan, 1974; Leventhal, 1983; Calvert and Karlin, 1991).

5.2. Sulfur isotopic composition of sedimentary pyrite

In the surface sediments at station 2 in front of the river Danube, relatively heavy $\delta^{34}S$ values ($-13.7‰$; $\sigma = 4.6‰$) were observed which differ significantly from the compositions at the stations 9, 10, 22 and 24 (Fig. 7). However, the apparent isotope fractionation is well within the range observed in experiments with pure sulfate-reducing bacteria (Chambers and Trudinger, 1979). Experimental studies have shown that sulfur isotope fractionation decreases with increasing cellular sulfate reduction rate (e.g., Kaplan and Rittenberg, 1964; Chambers and Trudinger, 1979). Therefore, the data at station 2 suggest that the cellular rates of microbial sulfate reduction or sediment accumulation rates were probably high when compared to the other stations. Additionally, the sediment at station 2 was (partially) closed to bottom water sulfate, as indicated by a decrease in pore water sulfate with depth (Fig. 3). The pore water profile of the other station in front of a river delta (station 13) also shows a distinct decrease in sulfate with sediment depth, suggesting that sulfate reduction out competes sulfide oxidation and sulfate resupply by diffusion. In a (partially) closed system, the diffusive transport processes are not sufficient to prevent a depletion of the sulfate pool with depth, resulting in an increase in the $\delta^{34}S$ value for the remaining sedimentary sulfate pool and consequently in the produced sulfide (Hartmann and Nielsen, 1969). As a result, the apparent isotope fractionation with respect to seawater will decrease. Also, the openness of the sediments with respect to sulfide could affect the isotopic composition of the sediment (Jørgensen, 1979). If all sulfide produced by sulfate reduction is trapped as pyrite immediately and buried permanently in the sediments, the system is closed with respect to sulfide. Conversely, if most of the produced sulfide is re-oxidized in the upper sediment layers, the sediment experiences open system diagenesis with respect to sulfate (Jørgensen, 1979). In general, large apparent isotopic fractionations are often associated with open systems or small extents of sulfate reduction in restricted systems, while small differences in isotopic composition between seawater sulfate and pyrite are an indication for a (partially) closed diagenesis system of sulfur. The isotopic composition of dissolved species may additionally be influenced by preferential diffusion of $^{32}SO_4^{2-}$ into the sediment (Jørgensen, 1979; Goldhaber and Kaplan, 1974; Chanton and Martens, 1987). Although the diffusion coefficients for $^{32}SO_4^{2-}$ and $^{34}SO_4^{2-}$ are almost the same (Trudinger, personal communication in Jørgensen, 1979; Piel and Böttcher, unpublished experimental data), the concentration gradient of $^{32}SO_4^{2-}$ could be higher due to the preferential microbial consumption of $^{32}SO_4^{2-}$ in the sediments. A similar reasoning applies for the diffusion of dissolved sulfide into the water column (Chanton et al., 1987; Chanton and Martens, 1987).

Several factors could cause the (partial) closed diagenesis system for sulfur at the coastal stations. Since the rivers discharge large amounts of suspended solids, the sedimentation rates are high in this area. These high deposition rates could restrict the exchange of sulfate. Also, high sulfate reduction rates in these coastal sediments could reduce the openness of the system for sulfate for it being determined by the balance between consumption and replenishment (Zaback et al., 1993). The relatively high SCOC rates recorded at stations 2 and 13 (37.9 and 26.3 mmol O_2 m^{-2} day^{-1}, respectively) suggest a high sulfate reduction activity in these sediments. Finally, the availability of large amounts of reactive iron in these sediments (Fig. 2; Wijsman et al., 2001b) could support high sulfide retention and thus cause low apparent isotopic fractionation. The reactive iron will trap most of the produced sulfide in the form of iron sulfides preventing re-oxidation of sulfide after diffusion to the oxidized upper sediment layers. Bioturbating organisms may additionally have influenced the depth variation in the isotopic composition of pyrite.

In the central part of the continental shelf (stations 9 and 10), the $\delta^{34}S$ values are very light (−38.5‰ to −46.3‰). These results are comparable to data from Vaynshteyn et al. (1986), who report a value of −45‰ in the upper 10 cm of a station located in the southern part of the northwestern continental shelf. Assuming that the $\delta^{34}S$ value of the sulfate in the near bottom water of the continental shelf is equal to sulfate in the upper 200 m of the deep sea (i.e., +19‰, Sweeney and Kaplan, 1980), this corresponds to an apparent maximum isotope fractionation of 65‰ at the central shelf stations. In an open system, (bio-enhanced) transport processes can be faster than the microbial rate of sulfate reduction (Jørgensen, 1979; Chanton et al., 1987). As a result, the sulfate concentration in the sediment will not decrease, and its isotopic composition will not change due to sulfate reduction. In such an open system, the apparent and instantaneous isotope fractionations are the same. The light isotopic values at stations 9 and 10 and the more or less constant concentrations of sulfate with depth, therefore, indicate that the sediments were open with respect to sulfate. The abundance of bio-irrigating benthic fauna in this area (Wijsman et al., 1999) might have enhanced the openness of these sediments for sulfate due to enhanced sulfate transport and enhanced re-oxidation. The magnitude of isotopic fractionation at stations 9 and 10, however, is extremely high when compared to the results of experimental studies. Laboratory experiments with pure-cultures of sulfate-reducing bacteria yielded isotope enrichment factors up to a maximum of 46‰ (Kaplan and Rittenberg, 1964). This indicates that isotope discrimination was not controlled by microbial sulfate reduction alone and thus that additional processes may have contributed to the observed overall isotope effect. Re-oxidation of H_2S leads to the formation of sulfur species with intermediate oxidation states, such as elemental sulfur and thiosulfate (Zhang and Millero, 1993). Whereas only minor isotope fractionation seems to occur during oxidation of H_2S (Fry et al., 1986), the microbial disproportionation of the sulfur intermediate has experimentally been shown to produce isotopically light H_2S (Canfield and Thamdrup, 1994;

Cypionka et al., 1998; Habicht et al., 1998), thus increasing the net isotope discrimination between sulfate and H_2S. In sediments that are open to the supply of oxidants, repetitive cycles of sulfate reduction, oxidation and disproportionation have been suggested to result in progressively lighter isotopic sulfur values (Canfield and Thamdrup, 1994). Moreover, complete oxidation of H_2S also results in depleted sulfate and once re-reduced, the resulting H_2S can have very low $\delta^{34}S$.

Significant variability with a steep downcore increase in the $\delta^{34}S$ values was observed in the profile of station 24 (Fig. 7). This trend is in agreement with data of Vaynshteyn et al. (1986) for shelf sediments near the oxic–anoxic interface. At present, there is no indication for a limited supply of dissolved sulfate and a related “reservoir effect” (Jørgensen, 1979) on the isotopic composition of pyrite because the sulfate concentrations remained nearly constant with depth (Fig. 5). We, therefore, suggest that the observed increase in $\delta^{34}S$ values has to be attributed to a non-steady state process where the system was more restricted (and reducing) in a previous period. A high carbon input or a high sedimentation rate in the past may have restricted the penetration of sulfate into the sediments. However, we are not aware of any evidence for an abrupt decrease in sedimentation rate and/or carbon flux to the sediment in this area in a previous period. Also, a switch between oxic and anoxic conditions of the near bottom water could affect the openness of the system for sulfate. Under low-oxygen to anoxic conditions, re-oxidation of reduced sulfide and thus sulfate re-supply in the sediment is low, which enhances the closed behavior of the system and limits the substrate for the activity of disproportionating bacteria. Moreover, anoxic conditions could reduce the bio-irrigation activity of the benthic fauna and so further decrease the openness of the system with respect to sulfate transport (Jørgensen, 1979; Chanton and Martens, 1987). It is possible that as a result of the long-term fluctuations of the oxic–anoxic interface (Lyons et al., 1993), the bottom water at this station changed from anoxic to oxic, which caused more depleted $\delta^{34}S$ values in the upper part of the sediment column because the re-oxidation cycle with its consequent fractionation was activated. As discussed in the previous section, the AVS profile at station 24 also supports a recent change from anoxic to oxic conditions of the bottom water at this station or a change in sedimentation rates.

Isotope results for pyrite in sediments from the deep-sea station 22 are light ($-37.0‰$ to $-38.9‰$) and compare well with the results of previous studies on deep-sea surface sediments of the Black Sea (Table 2). They are similar to the isotopic composition of H_2S near the chemocline or close to the sediment–water interface (Table 2; Fry et al., 1991; Sweeney and Kaplan, 1980; Neretin et al., 1998, 2001) and pore waters of deep-sea surface sediments (Neretin et al., 2001; Sweeney and Kaplan, 1980). It has previously been argued that the isotopic composition of deep-sea sediments is indicative for pyrite formation in the water column (Calvert et al., 1996; Lyons, 1997). From the compiled data for deep-water column and pore water H_2S in Table 2, however, it is clear that part of the pyrite may also form in the surface sediments of the deep sea, in agreement with balance calculations by Lyons (1997) and Neretin et al. (2001). Data on suspended particle composition in the anoxic water column (Cutter and Kluckhohn, 1999) indicate that significant concentrations of AVS are present in the near bottom water of the deep sea. These components would act as precursors for pyrite formation at these depths. The extremely light $\delta^{34}S$ values of H_2S in the anoxic water column have been attributed to internal recycling of sulfur (Canfield and Thamdrup, 1994). Elemental sulfur, which is extensively formed by oxidation of hydrogen sulfide near the chemocline (Jørgensen et al., 1991; Luther et al., 1991), settles through the water column where it might react with H_2S to form polysulfides, or be subjected to bacterial disproportionation, resulting in more negative values of the reduced sulfur pool (Canfield and Thamdrup, 1994; Raiswell, 1997; Canfield et al., 1998). Unfortunately, there are only very limited isotope data available for sulfur intermediates from the anoxic water column (Neretin et al., 1998, 2001) and no measurements have been made on samples from the chemocline. Sulfur intermediates, expressed as elemental sulfur and thiosulfate, closely follow the isotopic composition of H_2S (Table 2), indicating isotope exchange reactions or small fractionations during oxidation to occur. The S^0 data may additionally be explained by microbial reduction with depth (Kaplan and Rittenberg, 1964;

Böttcher and Surkov, unpublished experimental data). The present study demonstrates that pyrite which is extremely depleted in ^{34}S can be found in the Black Sea surface sediments positioned both above and below the chemocline, in spite of different biogeochemical and microbial controlling factors.

The upper slope sediments are a major source for the turbidite mud layers observed on the abyssal plain of the Black Sea (Lyons, 1997). During earth quake-related events, FeS-rich upper slope sediments can be transported to the deep-sea where the FeS may react with the H_2S present in the near bottom water to pyrite. According to the model of Lyons (1997), δ^{34}S values of turbidite sediments are therefore determined by both the concentration and isotopic composition of the FeS and pyrite in the upper slope sediments and the δ^{34}S-value of H_2S in the deep anoxic water (Fry et al., 1991; Neretin et al., 1998). In the model of Lyons (1997), the upper slope muds were assumed to be relatively constant in contents and δ^{34}S values of AVS (152 μmol S g^{-1}; -25.0‰) and pyrite (90 μmol S g^{-1}; -27.6‰).

In contrast, the present study demonstrates that shelf and upper slope sediments in the Black Sea are highly variable in AVS and pyrite contents and sulfur isotope compositions. This might indicate that the provenance of turbiditic muds is restricted to part of the slope area.

Acknowledgements

The authors thank the captain and the crew of the R.V. Prof. Vodyanitsky and Nicolae Panin who was in charge of the expedition. Eric Boschker, Peter van Breugel, Filip Meijsman and Pieter van Rijswijk assisted in the field and with the analysis in the laboratory. MEB wishes to thank Prof. Dr. J. Rullkötter for access to the isotope mass spectrometer of the Institute of Chemistry and Biology of the Marine Environment (ICBM, University of Oldenburg). Stable isotope measurements were supported by Max Planck Society, Munich. We thank Steve Calvert, and in particular Tim Lyons, for constructive reviews. This is a contribution 217 from the EROS-21 project of the Environment and Climate Program of the European Communities (ENV4-CT96-0286) to the ELOISE program. This is publication no. 2776 of the Netherlands Institute of Ecology, Yerseke.

References

Aller, R.C., 1988. Benthic fauna and biogeochemical processes in marine sediments: the role of burrow structures. In: Blackburn, T.H. (Ed.), Nitrogen Cycling in Coastal Marine Environments. Wiley, Chichester, pp. 301–338.

Aller, R.C., Rude, P.D., 1988. Complete oxidation of solid phase sulfides by manganese and bacteria in anoxic marine sediments. Geochimica et Cosmochimica Acta 52, 751–765.

Bagarinao, T., 1992. Sulfide as an environmental factor and toxicant: tolerance and adaptations in aquatic organisms. Aquatic Toxicology 24, 21–62.

Berner, R.A., 1970. Sedimentary pyrite formation. American Journal of Science 268, 1–23.

Berner, R.A., 1982. Burial of organic carbon and pyrite sulfur in the modern ocean: its geochemical and environmental significance. American Journal of Science 282, 451–473.

Berner, R.A., 1984. Sedimentary pyrite formation: an update. Geochimica et Cosmochimica Acta 48, 605–615.

Berner, R.A., Raiswell, R., 1983. Burial of organic carbon and pyrite sulfur in sediments over Phanerozoic time: a new theory. Geochimica et Cosmochimica Acta 47, 855–862.

Berner, R.A., Westrich, J.T., 1985. Bioturbation and the early diagenesis of carbon and sulfur. American Journal of Science 285, 193–206.

Boesen, C., Postma, D., 1988. Pyrite formation in anoxic environments of the Baltic. American Journal of Science 288, 575–603.

Böttcher, M.E., Smock, A., Cypionka, H., 1998a. Sulfur isotope fractionation during experimental precipitation of iron(II) and manganese(II) sulfide at room temperature. Chemical Geology 146, 127–134.

Böttcher, M.E., Oelschläger, B., Höpner, T., Brumsack, H.J., Rullkötter, J., 1998b. Sulfate reduction related to the early diagenetic degradation of organic matter and "black spot" formation in tidal sandflats of the German Wadden Sea (southern North Sea): stable isotope (^{13}C, ^{34}S, ^{18}O) and other geochemical results. Organic Geochemistry 29, 1517–1530.

Böttcher, M.E., Schale, H., Schnetger, B., Wallmann, K., Brumsack, H.J., 2000. Stable sulfur isotopes indicate net sulfate reduction in near-surface sediments of the deep Arabian Sea. Deep-Sea Research II 47, 2769–2783.

Calvert, S.E., Karlin, R.E., 1991. Relationships between sulphur, organic carbon, and iron in the modern sediments of the Black Sea. Geochimica et Cosmochimica Acta 55, 2483–2490.

Calvert, S.E., Thode, H.G., Yeung, D., Karlin, R.E., 1996. A stable isotope study of pyrite formation in the late Pleistocene and Holocene sediments of the Black Sea. Geochimica et Cosmochimica Acta 60, 1261–1270.

Canfield, D.E., 1988. Sulfate reduction and the diagenesis of iron in anoxic marine sediments. PhD Thesis, Yale University 248 pp.

Canfield, D.E., 1989. Sulfate reduction and oxic respiration in marine sediments: implications for organic carbon preservation in euxinic environments. Deep-Sea Research 36, 121–138.

Canfield, D.E., Thamdrup, B., 1994. The production of ^{34}S-depleted sulfide during bacterial disproportionation to elemental sulfur. Science 266, 1973–1975.

Canfield, D.E., Raiswell, R., Westrich, J.T., Reaves, C.M., Berner, R.A., 1986. The use of chromium reduction in the analysis of reduced inorganic sulfur in sediments and shales. Chemical Geology 54, 149–155.

Canfield, D.E., Thamdrup, B., Hansen, J.W., 1993a. The anaerobic degradation of organic matter in Danish coastal sediments: iron reduction, manganese reduction, and sulfate reduction. Geochimica et Cosmochimica Acta 57, 3867–3883.

Canfield, D.E., Jørgensen, B.B., Fossing, H., Glud, R.N., Gundersen, J., Ramsing, N.B., Thamdrup, B., Hansen, J.W., Nielsen, L.P., Hall, P.O.J., 1993b. Pathways of organic carbon oxidation in three continental margin sediments. Marine Geology 113, 27–40.

Canfield, D.E., Thamdrup, B., Fleischer, S., 1998. Isotope fractionation and sulfur metabolism by pure and enrichment cultures of elemental sulfur-disproportionating bacteria. Limnology and Oceanography 43, 253–264.

Chambers, L.A., Trudinger, P.A., 1979. Microbial fractionation of stable sulfur isotopes: a review and critique. Geomicrobiology Journal 1, 249–293.

Chanton, J.P., Martens, C.S., 1987. Biogeochemical cycling in an organic-rich coastal marine basin. 8. A sulfur isotopic budget balanced by differential diffusion across the sediment–water interface. Geochimica et Cosmochimica Acta 51, 1201–1208.

Chanton, J.P., Martens, C.S., Goldhaber, M.B., 1987. Biogeochemical cycling in an organic-rich coastal marine basin. 7. Sulfur mass balance, oxygen uptake and sulfide retention. Geochimica et Cosmochimica Acta 51, 1187–1199.

Cline, J.D., 1969. Spectrophotometric determination of hydrogen sulfide in natural waters. Limnology and Oceanography 14, 454–458.

Codispoti, L.A., Friederich, G.E., Murray, J.W., Sakamoto, C.M., 1991. Chemical variability in the Black Sea-implications of continuous vertical profiles that penetrated the oxic anoxic interface. Deep-Sea Research 38, S691–S710.

Cutter, G.A., Kluckhohn, R.S., 1999. The cycling of particulate carbon, nitrogen, sulfur and sulfur species (iron monosulfide, greigite, pyrite, and organic sulfur) in the water columns of Framvaren Fjord and the Black Sea. Marine Chemistry 67, 149–160.

Cypionka, H., Smock, A.M., Böttcher, M.E., 1998. A combined pathway of sulfur compound disproportionation in *Desulfovibrio desulfuricans*. FEMS Microbiology Letters 166, 181–186.

Dimitrov, P.S., Stoyanov, A.S., Demirov, E.K., Solakov, D.P., 1987. On the phenomenon of upwelling in the western part of the Black Sea and its connection with the bloom of plankton. Bulgarian Academy of Sciences 40, 127–130.

Fabry, V., Froehlich, K., Osvath, I., 1993. Environmental pollution of the Black Sea: a search for answers. International Atomic Agency Bulletin 35, 20–24.

Fossing, H., Jørgensen, B.B., 1989. Measurement of bacterial sulfate reduction in sediments: evaluation of a single-step chromium reduction method. Biogeochemistry 8, 205–222.

Fossing, H., Jørgensen, B.B., 1990. Oxidation and reduction of radiolabeled inorganic sulfur compounds in an estuarine sediment, Kysing Fjord, Denmark. Geochimica et Cosmochimica Acta 54, 2742.

Fry, B., Cox, J., Gest, H., Hayes, J.M., 1986. Discrimination between ^{34}S and ^{32}S during bacterial metabolism of inorganic sulfur compounds. Journal of Bacteriology 165, 328–330.

Fry, B., Jannasch, H.W., Molyneaux, S.J., Wirsen, C.O., Muramoto, J.A., King, S., 1991. Stable isotope studies of the carbon, nitrogen and sulfur cycles in the Black Sea and the Cariaco Trench. Deep-Sea Research 38, S1003–S1019.

Gagnon, C., Mucci, A., Pelletier, É., 1995. Anomalous accumulation of acid-volatile sulphides (AVS) in a coastal marine sediment, Saguenay Fjord, Canada. Geochimica et Cosmochimica Acta 59, 2663–2675.

Goldhaber, M.B., Kaplan, I.R., 1974. The sulfur cycle. In: Goldberg, E.D. (Ed.), Marine Chemistry. Wiley, New York, pp. 569–655.

Goldhaber, M.B., Aller, R.C., Cochran, J.K., Rosenfeld, J.K., Martens, C.S., Berner, R.A., 1977. Sulfate reduction, diffusion, and bioturbation in Long Island Sound sediments: report of the FOAM group. American Journal of Science 277, 193–237.

Guieu, C., Martin, J.M., Tankéré, S.P.C., Mousty, F., Trincherini, P., Bazot, M., Dai, M.H., 1998. On trace metal geochemistry in the Danube River and the Western Black Sea. Estuarine, Coastal and Shelf Science 47, 471–485.

Habicht, K., Canfield, D., Rethmeier, J., 1998. Sulfur isotope fractionation during bacterial reduction and disproportionation of thiosulfate and sulfite. Geochimica et Cosmochimica Acta 62, 2585–2595.

Hartmann, M., Nielsen, H., 1969. δ^{34}S-Werte in rezenten Meeressedimenten und ihre Deutung am Beispiel einiger Sedimentprofile aus der westlichen Ostsee. Geologische Rundschau 58, 621–655.

Heip, C.H.R., Goossen, N.K., Herman, P.M.J., Kromkamp, J., Middelburg, J.J., Soetaert, K., 1995. Production and consumption of biological particles in temperate tidal estuaries. Oceanography and Marine Biology: An Annual Review 33, 1–149.

Henneke, E., Luther, G.W., De Lange, G.J., 1991. Determination of inorganic sulfur speciation with polarographic techniques: some preliminary results for recent hypersaline anoxic sediments. Marine Geology 100, 115–123.

Henneke, E., Luther, G.W., De Lange, G.J., Hoefs, J., 1997. Sulphur speciation in anoxic hypersaline sediments from the eastern Mediterranean Sea. Geochimica et Cosmochimica Acta 61, 307–321.

Henrichs, S.M., Reeburgh, W.S., 1987. Anaerobic mineralization of marine sediment organic matter: rates and the role of anaerobic processes in the oceanic carbon economy. Geomicrobiology Journal 5, 191–238.

Hurtgen, M.T., Lyons, T.W., Ingall, E.D., Cruse, A.M., 1999. Anomalous enrichments of iron monosulfide in euxinic marine sediments and the role of H_2S in iron sulfide transformations:

examples from Effingham Inlet, Orca Basin and the Black Sea. American Journal of Science 299, 556–588.

Jørgensen, B.B., 1977. The sulfur cycle of a coastal marine sediment (Limfjorden, Denmark). Limnology and Oceanography 22, 814–832.

Jørgensen, B.B., 1979. A theoretical model of stable sulfur isotope distribution in marine sediments. Geochimica et Cosmochimica Acta 43, 363–374.

Jørgensen, B.B., 1982. Mineralization of organic matter in the sea bed—the role of sulfate reduction. Nature 296, 643–645.

Jørgensen, B.B., 1983. Processes at the sediment–water interface. In: Bolin, B. (Ed.), The Major Biogeochemical Cycles and their Interactions. Wiley, New York, pp. 477–509.

Jørgensen, B.B., Fossing, H., Wirsen, C.O., Jannasch, H.W., 1991. Sulfide oxidation in the anoxic Black Sea chemocline. Deep-Sea Research 38, S1083–S1103.

Kaplan, I.R., Rittenberg, R.C., 1964. Microbiological fractionation of sulphur isotopes. Journal of General Microbiology 34, 195–212.

Kempe, S., Liebezeit, G., Diercks, A.R., Asper, V., 1990. Water balance in the Black Sea. Nature 346, 419.

Kostka, J.E., Luther, G.W., 1994. Partitioning and speciation of solid phase iron in saltmarsh sediments. Geochimica et Cosmochimica Acta 58, 1701–1710.

Kostka, J.E., Thamdrup, B., Glud, R.N., Canfield, D.E., 1999. Rates and pathways of carbon oxidation in permanently cold Arctic sediments. Marine Ecology Progress Series 180, 7–21.

Leventhal, J.S., 1983. An interpretation of carbon and sulfur relationships in Black Sea sediments as indicators of environmental deposition. Geochimica et Cosmochimica Acta 47, 133–137.

Lin, S., Morse, J.W., 1991. Sulfate reduction and iron sulfide mineral formation in Gulf of Mexico anoxic sediments. American Journal of Science 291, 55–89.

Luther, G.W., 1991. Pyrite synthesis via polysulfide compounds. Geochimica et Cosmochimica Acta 55, 2839–2849.

Luther, G.W., Church, T.M., Powell, D., 1991. Sulfur speciation and sulfide oxidation in the water column of the Black Sea. Deep-Sea Research 38, S1121–S1137.

Lyons, T.W., 1997. Sulfur isotopic trends and pathways of iron sulfide formation in upper Holocene sediments of the anoxic Black Sea. Geochimica et Cosmochimica Acta 61, 3367–3382.

Lyons, T.W., Berner, R.A., 1992. Carbon–sulfur–iron systematics of the uppermost deep-water sediments of the Black Sea. Chemical Geology 99, 1–27.

Lyons, T.W., Berner, R.A., Anderson, R.F., 1993. Evidence for large pre-industrial perturbations of the Black Sea chemocline. Nature 365, 538–540.

Martin, J.M., Windom, H.L., 1991. Present and future roles of ocean margins in regulating marine biogeochemical cycles of trace elements. In: Mantoura, R.F.C. (Ed.), Ocean Margin Processes in Global Change. Wiley, New York, pp. 45–67.

Mee, L.D. et al., 1992. The Black Sea in crisis: a need for concerted international action. Ambio 21, 278–286.

Middelburg, J.J., 1991. Organic carbon, sulphur, and iron in recent semi-euxinic sediments of Kau Bay, Indonesia. Geochimica et Cosmochimica Acta 55, 815–828.

Middelburg, J.J., Calvert, S.E., Karlin, R.E., 1991. Organic-rich transitional facies in silled basins: response to sea-level change. Geology 19, 679–682.

Muramoto, J.A., Honjo, S., Fry, B., Hay, B.J., Howarth, R.W., Cisne, J.L., 1991. Sulfur, iron and organic carbon fluxes in the Black Sea-sulfur isotopic evidence for origin of sulfur fluxes. Deep-Sea Research 38, S1151–S1187.

Neretin, N., Böttcher, M.E., Volkov, I.I., 1998. The stable sulfur isotopic composition of sulfur species in the Black Sea water column. Mineralogical Magazine 62A, 1075–1076.

Neretin, N., Volkov, I.I., Böttcher, M.E., Grinenko, V.A., 2001. A sulfur budget for the Black Sea anoxic zone. Deep-Sea Research I, submitted for publication.

Passier, H., Middelburg, J.J., Van Os, B.J.H., De Lange, G.J., 1996. Diagenetic pyritisation under eastern Mediterranean sapropels caused by downward sulphide diffusion. Geochimica et Cosmochimica Acta 60, 751–763.

Passier, H., Middelburg, J.J., De Lange, G.J., Böttcher, M.E., 1999. Modes of sapropel formation in the eastern Mediterranean: some constraints based on pyrite properties. Marine Geology 153, 199–219.

Popa, A., 1993. Liquid and sediment inputs of the Danube river into the north-western Black Sea. Mitteilungen aus dem Geologisch-Paleontologischen Intitut der Universität Hamburg 74, 137–149.

Price, F.T., Shieh, Y.N., 1979. Fractionation of sulfur isotopes during laboratory synthesis of pyrite at low temperatures. Chemical Geology 27, 245–253.

Raiswell, R., 1997. A geochemical framework for the application of stable sulfur isotopes to fossil pyritization. Journal of the Geological Society, London 154, 343–357.

Raiswell, R., Canfield, D.E., 1998. Sources of iron for pyrite formation in marine sediments. American Journal of Science 298, 219–245.

Raiswell, R., Canfield, D., Berner, R.A., 1994. A comparison of iron extraction methods for the determination of degree of pyritisation and the recognition of iron-limited pyrite formation. Chemical Geology 111, 101–110.

Rickard, D.T., 1995. Kinetics of FeS precipitation: Part 1. Competing reaction mechanisms. Geochimica et Cosmochimica Acta 59, 4367–4379.

Rickard, D.T., 1997. Kinetics of pyrite formation by the H_2S oxidation of iron (II) monosulfide in aqueous solutions between 25 and 125°C: the mechanism. Geochimica et Cosmochimica Acta 61, 135–147.

Shaffer, G., 1986. Phosphate pumps and shuttles in the Black Sea. Nature 321, 515–517.

Sinninghe Damste, J., De Leeuw, J.W., 1990. Analysis, structure and geochemical significance of organically-bound sulphur in the geosphere: state of the art and future research. Organic Geochemistry 16, 1077–1101.

Sorokin, Y.I., 1983. The Black Sea. In: Ketchum, B.H. (Ed.), Estuaries and Enclosed Seas. Elsevier, New York, pp. 253–292.

Stookey, L.L., 1970. Ferrozine—a new spectrophotometric reagent for iron. Analytical Chemistry 42, 779–781.

Sweeney, R.E., Kaplan, I.R., 1980. Stable isotope composition of dissolved sulfate and hydrogen sulfide in the Black Sea. Marine Chemistry 9, 145–152.

Thamdrup, B., Canfield, D.E., 1996. Pathways of carbon oxidation in continental margin sediments off central Chile. Limnology and Oceanography 41, 1629–1650.

Tolmazin, D., 1985. Changing coastal oceanography of the Black Sea. I: Northwestern shelf. Progress in Oceanography 15, 217–276.

Vaynshteyn, M.B., Tokarev, V.G., Shakola, V.A., Lein, A.Y., Ivanov, M.V., 1986. The geochemical activity of sulfate-reducing bacteria in sediments in the western part of the Black Sea. Geochemistry International 23, 110–122.

Wijsman, J.W.M., Herman, P.M.J., Gomoiu, M.T., 1999. Spatial distribution in sediment characteristics and benthic activity on the northwestern Black Sea shelf. Marine Ecology Progress Series 181, 25–39.

Wijsman, J.W.M., Herman, P.M.J., Middelburg, J.J., Soetaert, K., 2001a. A model for early diagenetic processes in sediments of the continental shelf of the Black Sea. Estuarine, Coastal and Shelf Science (In Press).

Wijsman, J.W.M., Middelburg, J.J., Heip, C.H.R., 2001b. Reactive iron in Black Sea sediments: implications for iron cycling. Marine Geology 172, 167–180.

Wilkin, R.T., Arthur, M.A., Dean, W.E., 1997. History of water-column anoxia in the Black Sea indicated by pyrite framboid size distributions. Earth and Planetary Science Letters 148, 517–525.

Zaback, D.A., Pratt, L.M., Hayes, J.M., 1993. Transport and reduction of sulfate and immobilization of sulfide in black shales. Geology 21, 141–144.

Zaitsev, Y.P., 1993. Impacts of eutrophication on the Black Sea fauna. Anonymous,Fisheries Council for the Mediterranean. Studies and Reviews, FAO, Rome, pp. 63–86.

Zhabina, N.N., Volkov, I.I., 1978. A method of determination of various sulfur compounds in sea sediments and rocks. In: Krumbein, W.E. (Ed.), Methods, Metals and Assessment. Ann Arbor Sci. Publ., MI, pp. 735–746.

Zhang, J.Z., Millero, F.J., 1993. The products from the oxidation of H_2S in seawater. Geochimica et Cosmochimica Acta 57, 1705–1718.